

Structural and thermal characterization of dioctadecyldimethylammonium bromide dispersions by spin labels

Carlos R. Benatti ^a, Eloi Feitosa ^{a,*}, Roberto M. Fernandez ^b,
M. Teresa Lamy-Freund ^b

^a *Physics Department, IBILCE/UNESP, Rua Cristóvão Colombo, 2265 Sao Jose do Rio Preto SP, CEP 15054-000, Brazil*

^b *Instituto de Física, Universidade de S. Paulo, CP 66318, CEP 05315-970, S. Paulo, SP, Brazil*

Received 19 September 2000; received in revised form 22 January 2001; accepted 22 January 2001

Abstract

Dioctadecyldimethylammonium bromide (DODAB) dispersions obtained by simply mixing the amphiphile in water, and by bath-sonication, were investigated by electron spin resonance (ESR) of stearic acids and their methyl ester derivatives, labeled at the 5th and 16th carbons of the acyl chain. The ESR spectra indicate that the non-sonicated dispersions are formed mainly by one population of DODAB vesicles, either in the gel ($T < T_m$) or in the liquid–crystalline ($T > T_m$) state. Around T_m there is a co-existence of the two phases, with a thermal hysteresis of about 3.2°C. In sonicated DODAB dispersions, spin labels indicate two different environments even for temperatures far below T_m : one similar to that obtained with non-sonicated samples, a gel phase, and another one in the liquid–crystalline state. The fluid phase domain present below T_m could correspond to either the periphery of bilayer fragments, reported to be present in sonicated DODAB dispersions, or to high curvature vesicles. © 2001 Elsevier Science Ireland Ltd. All rights reserved.

Keywords: Dioctadecyldimethylammonium bromide; Spin label; Cationic vesicle; Thermal analyses; Melting temperature

1. Introduction

Since the first formation in 1977 of cationic unilamellar vesicles of long double-chain quaternary ammonium surfactants (Kunitake and Okahata, 1977), several methods have been used to

prepare stabilized vesicles with well-defined size distribution, which may be suitable as membrane mimetic systems (Fendler, 1982; Carmona-Ribeiro, 1992; Feitosa et al., 2000), catalysts (Kawamuro et al., 1991), drug delivery vehicles or carriers in gene therapy (Lasic, 1993). Several research groups have been investigating the properties of these synthetic vesicles, and searching new applications for them (Carmona-Ribeiro and Chaimovich, 1983; Cuccovia et al., 1990; Car-

* Corresponding author. Tel.: +55-17-2212238; fax: +55-17-2212247.

E-mail address: eloi@df.ibilce.unesp.br (E. Feitosa).

mona-Ribeiro, 1992; Engberts and Hoekstra, 1995; Cuccovia et al., 1997; Carvalho and Carmona-Ribeiro, 1998; Blandamer et al., 1999; Kikuchi and Carmona-Ribeiro, 2000).

It has been shown that the physical and morphological properties of dioctadecyldimethylammonium chloride (DODAC) or bromide vesicles (DODAX; X being C for Cl^- or B for Br^-), such as the degree of counterion dissociation, hydrodynamic radius, polydispersity and melting temperature, depend on the preparation protocol and the solvent conditions, including the presence of additives (Cuccovia et al., 1990; Feitosa and Brown, 1997; Benatti et al., 1999; Feitosa et al., 2000). Large unilamellar vesicles are formed by simply mixing DODAX with water, at low surfactant concentration (Blandamer et al., 1999; Feitosa et al., 2000). DODAX unilamellar vesicles with higher curvature are then prepared using one of the protocols available, such as extrusion or sonication, the latter being the most used method for preparing high curvature vesicles. Overall, the mean diameter of sonicated DODAX vesicles ranges from 20 to 100 nm, depending on the surfactant chemical structure, solvent composition or sonication conditions. Sonication, however, not only increases the vesicle curvature, but also forms smaller aggregates (with diameter less than 20 nm), possibly bilayer fragments (Liu et al., 1992; Feitosa and Brown, 1997) or lens-like structures (Andersson et al., 1995).

A number of techniques have been used to investigate the phase behavior of DODAX dispersions prepared by different methods. It includes turbidity (Nascimento et al., 1998), static light scattering (Feitosa and Brown, 1997), static fluorescence (Benatti et al., 1999), surface pressure (Gugliotti et al., 1998), differential scanning calorimetry (DSC) (Feitosa et al., 2000), and electron spin resonance (ESR; Liu et al., 1992). Though DSC is the preferred method for measuring the gel to liquid–crystalline phase transition temperature, T_m , several other techniques can give important complementary information on the thermal behavior of lipid systems. Below T_m , the hydrocarbon chains are in a more rigid and extended gel state, whereas above T_m they are in a more flexible and disordered liquid–crystalline

phase. Therefore, the cooperativity of the gel to liquid–crystalline phase transition may depend on the vesicle structure and curvature, which, in turn, are determined by the method of vesicle preparation, lipid composition and solvent conditions (ionic strength, pH, presence of additives, etc.). Fluorescence probes incorporated in DODAX aggregates showed that the dispersions prepared by simply mixing DODAX with water (here called non-sonicated dispersion) display a sharp temperature transition at $T_m \approx 42^\circ\text{C}$, indicating a highly cooperative gel to liquid–crystalline phase transition. The bath-sonicated samples exhibit a broader temperature transition profile, centered at a somewhat lower transition temperature (Benatti et al., 1999).

The ESR of spin labels incorporated in amphiphilic aggregates have been extensively used to monitor the viscosity and polarity of the microenvironment where the probes are localized (see, for instance, Schreier et al. (1978), Marsh (1981), and references therein). In the present work, we monitored by ESR two differently prepared dioctadecyldimethylammonium bromide (DODAB) dispersions, namely, non-sonicated and bath-sonicated, using four types of spin labels: stearic acid derivatives (SASL) and their methyl ester (MESL), labeled at the 5th and the 16th carbon of the acyl chain (5-SASL, 16-SASL, 5-MESL and 16-MESL). Although the labels display different degrees of hydrophobicity, they exhibit a low solubility in aqueous medium, thus incorporating in the DODAB aggregates. The amphiphiles labeled at the 5th carbon atom monitor the DODAB aggregates closer to their water interface, whereas the 16 C-atom labels give information about the bilayer core, close to the end of the DODAB hydrocarbon chains. Owing to their distinct chemical characteristics, the stearic acid (probably negatively charged in the cationic DODAB aggregates; Ptak et al., 1980) and the methyl ester derivatives (neutral and less polar than the acid) may partition diversely among the structurally different aggregates or bilayer domains present in the samples.

The ESR results presented here bring a new contribution to the understanding of the structure of the DODAB aggregates. They show that below

T_m , in sonicated dispersions, DODAB aggregates share a two-phase (gel and liquid-crystalline) state, whereas in non-sonicated dispersions the coexistence of the two phases is only observed close to the transition temperature. The results are discussed on the basis of the curvature and structure of the aggregates.

2. Materials and methods

2.1. Materials

DODAB from Eastman Kodak, and octadecyltrimethylammonium bromide ($C_{18}TAB$), from Fluka, were used as purchased. DODAC was obtained from DODAB by ion exchange and recrystallized as described elsewhere (Cuccovia et al., 1997). The 5- and 16-doxyl stearic acid spin labels (5- and 16-SASL) and their methyl ester derivatives, 5- and 16-MESL, were used as purchased from Sigma Chemical Co. Fig. 1 shows the molecular formula of 16-SALS. 5-SALS contains the doxyl group at the 5th C-atom, and the *n*-MELS has the H^+ replaced by the methyl ester group.

2.2. DODAB dispersions and $C_{18}TAB$ micelle preparation

Non-sonicated dispersions were prepared by mixing DODAB crystals with water at $58^\circ C$ (above T_m) to the final concentration of 5 mM. Bath-sonicated dispersions were obtained by sonicating the 5 mM DODAB dispersions with a Branson 1210 bath-type cell disrupter at $58^\circ C$. Fig. 2 shows the effect of bath-sonication time on the optical density (OD) of DODAB dispersions (time $t = 0$ corresponds to the non-sonicated dis-

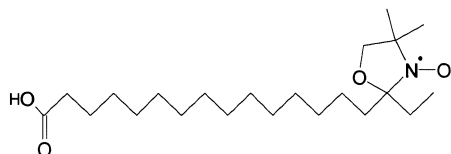


Fig. 1. Molecular formula of 16-doxyl stearic acid spin label (16-SASL).

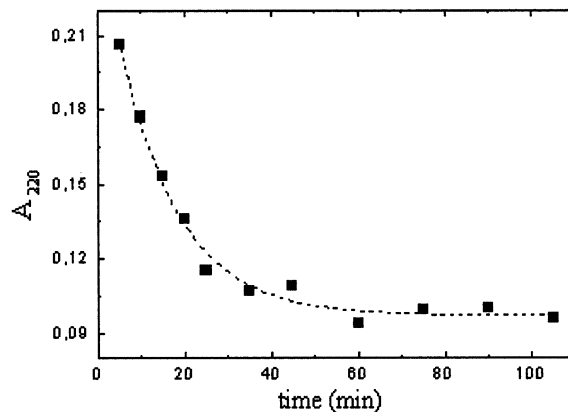


Fig. 2. Effect of bath-sonication time on the turbidity of DODAB aqueous dispersion. Measurements made at $\lambda = 220$ nm.

ersion). It clearly shows that after about 60 min sonication the turbidity attains a plateau, suggesting that the bilayer structures in the dispersion have reached a minimum size. We have sonicated the dispersions for 90 min, safely above the 60 min necessary to achieve the plateau. After preparation, the DODAB dispersions were stored at room temperature, and found to be stable for months, as monitored by light scattering (Feitosa and Brown, 1997). $C_{18}TAB$ micelles were prepared by simply mixing the surfactant crystals (5 mM) in water above the Krafft point of the surfactant ($\approx 38^\circ C$) and stored at room temperature. Turbidity measurements were made in an UV-visible spectrophotometer (Hitachi, model U-2001) equipped with two quartz square cells (1 cm of optical path-length) for vesicle and reference samples.

2.3. Spin labeled sample preparations

Films were formed from chloroform solutions of the spin labels, dried under a N_2 stream and left under reduced pressure for at least 2 h to remove all traces of the organic solvent. Spin labeled dispersions of DODAB and $C_{18}TAB$ were prepared by adding the amphiphilic dispersion to the dried film of spin labels (to a final concentration of no more than 0.8 mol% of label relative to amphiphile, to avoid spin-spin interactions), and

the sample smoothly stirred for 5 min. The ESR measurements were always started within 1 h after the addition of the spin labels to the dispersions.

2.4. ESR spectroscopy

ESR measurements were performed with a Bruker EMX spectrometer. Field-modulation amplitude of 1 G and microwave power of 5 mW were used. The temperature was controlled to about 0.2°C with a Bruker BVT-2000 variable temperature device, and monitored with a Fluke 51 K/J thermometer with the probe placed just above the cavity. The magnetic field was measured with a Bruker ER 035 NMR Gaussmeter, and, when desired, the spectra were converted to a *g*-value scale with the WINEPR software (Bruker).

2.5. ESR parameters

The empirical parameter A_{\max} is the maximum hyperfine splitting directly measured in the spectrum (Fig. 3), which increases with the label microenvironment viscosity and/or order (Freed, 1976). At high temperatures, the parameters of the ESR spectra of the more mobile probes, labeled at the 16th carbon atom, were found by fitting each line to a Gaussian–Lorentzian sum function (Halpern et al., 1993), taking advantage of the fact that the sum function is an accurate representation of a Gaussian–Lorentzian convolution, the Voigt function (Bales, 1989). Due to the difficulty in postulating a preferential rotational axis for the probes (Marsh, 1989), rotational correlation times, τ_B and τ_C , were calculated by the fitting of the ESR spectra, using the principal components of the *g* and hyperfine tensors of doxyl-propane, and 3300 G for the magnetic field (Schreier et al., 1978). The corrections for the contribution of non-resolved hyperfine splittings (Bales, 1989) were made. Considering that these two correlation times should be identical for rapid, isotropic movement, the movement asymmetry can be estimated by the τ_C/τ_B ratio. The isotropic hyperfine splitting, a_0 , was taken to be one-half the difference in the resonance fields of the high- and low-field lines, or

was directly measured in the spectra (see 16-MESL or 16-SASL spectra at high temperatures in Fig. 3). For anisotropic ESR spectra yielded by 5-SASL and 5-MESL, a_0 can be calculated from the principal values of the hyperfine tensor obtained by theoretical spectral simulation, $a_0 = (1/3)(A_{xx} + A_{yy} + A_{zz})$. For the ESR spectral simulations, we used the computer program NLSL developed by Freed and co-workers (Schneider and Freed, 1989; Budil et al., 1996; Ge and Freed, 1999). The parameters used have been extensively discussed in their papers, and the most relevant points for performing the simulations have been recently reviewed (Fernandez and Lamy-Freund, 2000). The *g*-tensor components

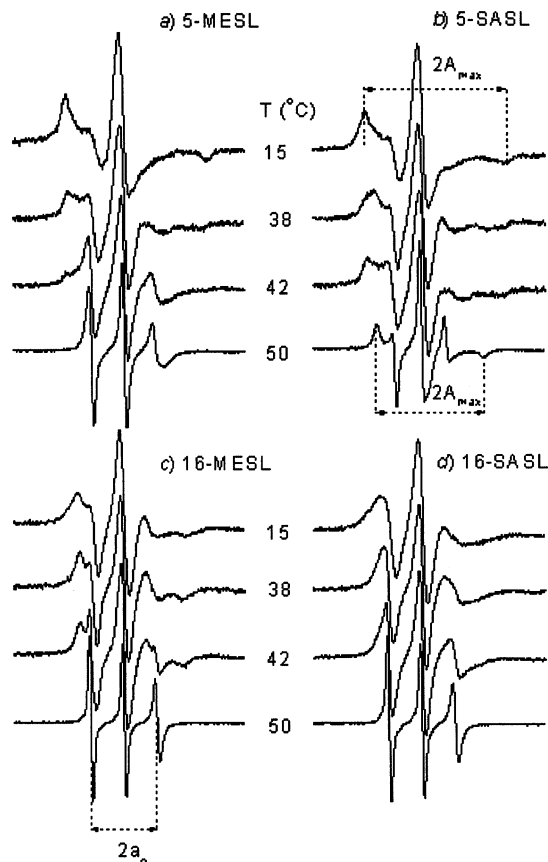


Fig. 3. ESR spectra of 5- and 16-MESL and SASL in non-sonicated DODAB dispersions at 15, 38, 42 and 50°C. Total spectra width 100 G. The outer hyperfine splitting (A_{\max}) and the isotropic hyperfine splitting (a_0) are indicated.

were kept as $g_{xx} = 2.0089$, $g_{yy} = 2.0058$ and $g_{zz} = 2.0021$ (Earle et al., 1994; Ge and Freed, 1999). The hyperfine splitting tensor was considered to be axial, $A_{xx} = A_{yy} = A_{\perp}$, and the A_{\perp} and A_{zz} values were allowed to vary within a reasonable interval (Earle et al., 1994). Rotational correlation times (τ_{\perp} and τ_{\parallel}) were calculated based on the best results obtained for the principal values of an axially symmetric rotational diffusion tensor for the nitroxide moiety attached to the chain segment. The microscopic orientational ordering of the spin label is characterized here by two terms of the restoring potential (Schneider and Freed, 1989), S_{20} and S_{22} , related to the amplitude of the rotational motion.

2.6. Relative vertical position of the SASL and MESL in DODAB bilayers

It is interesting to note that 5-SASL in DODAB aggregates monitors a highly ordered region, as indicated by the rather large A_{\max} value measured in the ESR signal (Fig. 3). Accordingly, the theoretical simulation of the 5-SASL signal at 50°C (dashed lines in Fig. 4(b)) indicates that its movement is relatively fast and highly ordered, as evidenced by the fairly low correlation times (mainly a low τ_{\parallel}) and high order parameters (S_{20} and S_{22} ; Table 1). The simulation of the 5-MESL signal (dashed lines in Fig. 4(a)) indicates that this label is localized in a less packed bilayer region, presenting lower correlation times and order parameters, relative to 5-SASL (Table 1). Therefore, assuming that the two label molecules incorporate in similar structural regions, and considering the known flexibility gradient towards the membrane center (Hubbell and McConnell, 1971), it can be concluded that, at 50°C, the SASL is localized in a shallower position in the bilayer than the MESL. Hence, for the former, both the correlation time and the order parameter measured in the ESR spectra of the N–O moiety are higher than those obtained for the methyl ester derivative. That is in accord with the somewhat larger isotropic hyperfine splitting, a_0 , obtained for 5-SASL as compared to 5-MESL (Table 1), indicating a microenvironment of higher dielectric constant for the N–O group in

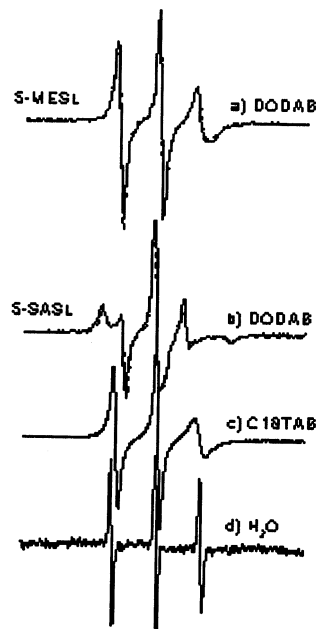


Fig. 4. ESR spectra of 5-MESL (a) and 5-SASL (b), (c) and (d) incorporated in liquid-crystalline non-sonicated DODAB aggregates (a) and (b), in C_{18} TAB micelles (c), and free in water (d). Computer simulations of the spectra (see text) are shown by dashed lines. The spectral parameters derived from the fits are given in Table 1. Temperature 50°C. Total spectra width 100 G.

the stearic acid (Griffith et al., 1974).¹ The stearic acid headgroup is possibly closer to the bilayer/water interface due to the electrostatic interaction between its negatively charged head group (Ptak et al., 1980) and the cationic surface of DODAB aggregates. The methyl group makes the *n*-MESL a very hydrophobic probe with a rather low polar headgroup. It is interesting to point out that in the lipid gel phase (15°C, Fig. 3) the labels relative position is inverted, as attested by the larger A_{\max} value yielded by 5-MESL ($A_{\max} = 61.4$ G) compared to that of 5-SASL ($A_{\max} = 60.4$ G).²

¹ It is important to note that a_0 values can only be relatively well evaluated for ESR signals typical of probes displaying fast movement, with correlation times lower than $\sim 10^{-9}$ s, therefore incorporated in fluid phase bilayers (for further discussion, see Fernandez and Lamy-Freund, 2000).

² The MESL vertical movement at bilayer phase transitions has been previously observed (Fernandez and Lamy-Freund, 2000; Turchiello et al., 2000) and should be taken into consideration when the information from the different labels is compared.

Table 1

Parameters obtained from non-linear least-squares fitting^a of the ESR spectra of 5-MESL and 5-SASL in DODAB dispersions at 50°C

	A_{\parallel} (G)	A_{zz} (G)	a_0 (G)	τ_{\parallel} (ns)	τ_{\perp} (ns)	S_{20}	S_{22}
5-MESL	5.12	33.84	14.69	0.028	0.61	0.12	-0.15
5-SASL	5.00	34.50	14.83	0.52	17	0.42	-0.57

^a For the discussion of the simulating program used and the spectral parameters, see Section 2. The experimental and theoretical spectra are shown in Fig. 4.

3. Results and discussion

3.1. Non-sonicated DODAB dispersions

The ESR spectra yielded by the labels 5- and 16-SASL, and 5- and 16-MESL, incorporated in non-sonicated DODAB dispersions, at four different temperatures, are shown in Fig. 3. Due to the flexibility gradient towards the bilayer core (Hubbell and McConnell, 1971), at a certain temperature, the spectra yielded by the 5th carbon labeled amphiphiles are much more anisotropic than those yielded by the probes labeled at the 16th carbon of the acyl chain, which monitor the bilayer core (Fig. 3). Yet, the ESR signals of all four labels can be interpreted as monitoring a highly packed environment at 15°C, typical of amphiphiles in the gel phase, and a much more mobile environment at 50°C, consistent with a bilayer liquid-crystalline state. In the intermediate temperatures, 38 and 42°C, the ESR spectra seem to be due to a mixture of these two phases with distinct degrees of fluidity (this point will be further discussed below).

At 50°C, above T_m , the spectra yielded by the 16 C-atom labels in DODAB non-sonicated dispersion are characteristic of the motionally narrowing region, with a low order parameter (Marsh, 1981). As expected, 5-MESL and 5-SASL, which monitor a relatively organized environment close to the bilayer surface, present anisotropic signals even at high temperatures (large A_{\max} values). The simulations shown in Fig. 4 strongly indicate that the bilayer domains present in non-sonicated DODAB dispersions are homogeneous, as the ESR spectrum of each spin

label can be fairly well simulated by a single signal.

It is important to note that the results obtained with spin labels incorporated in DODAB aggregates, namely, a highly ordered movement at the 5th position of the acyl chain together with a rather disordered movement at the 16th position, are typical of bilayer structures in the liquid-crystalline state, never yielded by micelles. For comparison, Fig. 4 shows the spectra of 5-SASL incorporated in micelles of the homologue surfactant C₁₈TAB and in water (c and d, respectively). It is evident from the ESR spectrum that 5-SASL in micelles (Fig. 4(c)) undergoes a much more isotropic movement than in DODAB aggregates (Fig. 4(b)), displaying three relatively narrow hyperfine lines, though much broader than those obtained for the spin label tumbling free in water (Fig. 4(d)).

As mentioned before, the ESR spectra of spin labels incorporated in non-sonicated DODAB aggregates at temperatures around 40°C (close to T_m) can be interpreted as the sum of two signals, corresponding to labels in different bilayer structural domains: a gel and a liquid-crystalline phase. This is an indication that the DODAB main phase transition occurs over a range of temperature, with the coexistence of the two phases³. Since the use of labels always brings

³ It is interesting to point out that the fact that two well-separated spectra are obtained shows that the exchange rate between the labels in the two different phase domains is slow on the ESR time scale (lower than about 10^8 s⁻¹). This is more evident for the 16-MESL than for the other spin labels used.

Table 2

Parameters obtained from the fitting of the ESR spectra of 16-MESL and 16-SASL in different samples at 50°C^a

Sample	16-MESL			16-SASL		
	τ_B (ns)	τ_C (ns)	a_0 (G)	τ_B (ns)	τ_C (ns)	a_0 (G)
NS-DODAB ^b	0.38	0.28	14.35	0.45	0.35	14.24
SO-DODAB ^c	0.37	0.31	14.40	0.49	0.42	14.37
C ₁₈ TAB	0.21	0.20	14.90	0.15	0.16	14.96
H ₂ O	–	–	–	0.04	0.04	15.75

^a For the discussion of the spectral parameters, see Section 2.

^b Non-sonicated DODAB dispersion.

^c Sonicated DODAB dispersion. The estimated errors for τ and a_0 are around ± 0.03 ns and ± 0.03 G, respectively.

some uncertainty about their exact location in the membrane, it is interesting to point out that the ESR parameter a_0 indicates that the more mobile signal is also yielded by the nitroxide moiety inside the hydrophobic bilayer core and not at the bilayer/water interface. For example, in the 16-MESL spectrum at 42°C (Fig. 3(c)), where the presence of the two different signals is rather evident, it is possible to estimate the value of the isotropic hyperfine constant of the more mobile signal by direct measurement at the ESR spectrum, $a_0 = 14.16$ G. This low value, compared to the one obtained with 16-SASL in aqueous solution at the same temperature, $a_0 = 15.73$ G (spectrum not shown), indicates that in DODAB dispersions, the spin labels responsible for the two different ESR signals are incorporated inside the aggregates. Moreover, the a_0 value obtained for the mobile signal at 42°C (14.16 G) is close to that yielded by the same sample at 50°C, in the fluid phase, $a_0 = 14.35$ (Table 2). (Usually, the a_0 values do not change much with temperature, varying less than 0.3% from 35 to 50°C, in aqueous solution).

Interestingly, the phase transition shows a hysteresis effect as indicated by the 16-MESL spectra in Fig. 5: at a given temperature, the DODAB bilayer is more fluid under cooling than heating. In order to monitor the phase transition, an empirical parameter is plotted versus the sample temperature (Fig. 6(a)). It is the ratio of the 16-MESL ESR spectrum amplitudes at positions b and a (Fig. 5), where a and b are mainly related to the gel and liquid–crystalline phases, respec-

tively. The gel to liquid–crystalline phase transition temperatures (T_m) were found to be around 39.5 and 42.7°C, under cooling and heating, respectively. No alteration in the two different ESR spectra obtained under heating or cooling the DODAB sample was observed up to 15 min of incubating the sample at 40°C, suggesting that in both cases the surfactant suspension is in a metastable equilibrium.

Another ESR parameter that can be used to monitor the thermal phase transition is the line width of the central field line, ΔH_0 (Fig. 5). Fig.

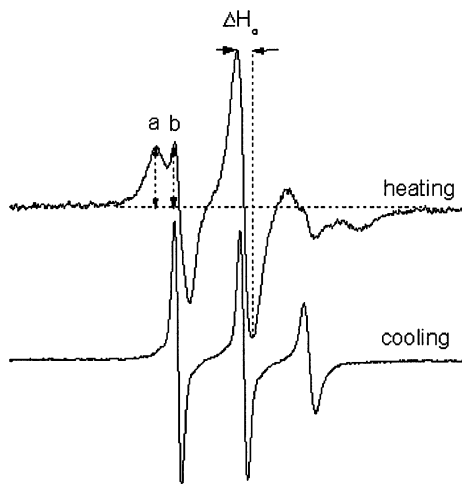


Fig. 5. The hysteresis effect in non-sonicated DODAB dispersions at 40°C, evidenced by the different 5-MESL ESR spectra obtained upon cooling and heating the sample. Total spectra width 100 G. (a) and (b) are the amplitudes at the two indicated positions. ΔH_0 is the line width of the central field line.

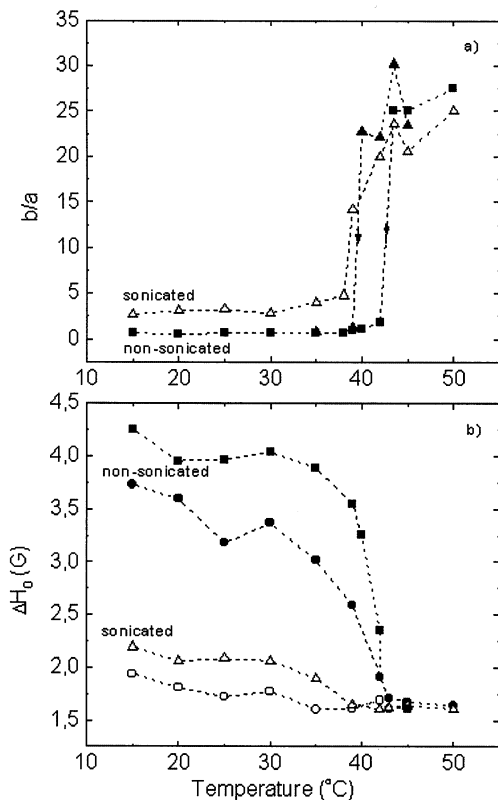


Fig. 6. Temperature dependence of the ratio b/a and the central field line width (ΔH_0 ; see Fig. 5). The parameters were measured in the ESR spectra of 16-MESL (Δ , \blacksquare , \square) and 16-SASL (\bullet , \circ), in non-sonicated (solid symbols) and sonicated (open symbols) DODAB dispersions. All but (\square) were obtained by heating the samples.

6(b) shows the ΔH_0 variation with temperature for both 16-MESL and 16-SASL incorporated in DODAB bilayers. As this is an average parameter, which does not distinguish the two lipid phases, the thermal transition seems to be slightly broader than when monitored by the b/a ratio in the 16-MESL spectra (Fig. 6(a); the 16-SASL monitors an even broader temperature transition, and the b/a ratio cannot be measured in the spectra). The information yielded by this parameter could be similar to those produced by the fluorescent probes that partition among the different bilayer domains, giving an average value of the membrane viscosity (Benatti et al., 1999). For instance, similar to the ESR results presented

here, steady-state fluorescence studies revealed a rather sharp (cooperative) main transition for DODAB in non-sonicated dispersions ($T_m \approx 42^\circ\text{C}$), but could not monitor the coexistence of the gel and the fluid phases around T_m (mainly monitored here by the b/a ratio of the 16-MESL ESR spectra).

3.2. Sonicated DODAB dispersions

Unlike the results for non-sonicated DODAB dispersions, spin labels incorporated in DODAB sonicated samples indicate the presence of two distinct lipid populations at 15°C (below T_m): one highly packed, probably in the gel state, and the other one rather mobile. Here, again, the low a_0 parameter measured in the 16-MESL mobile sig-

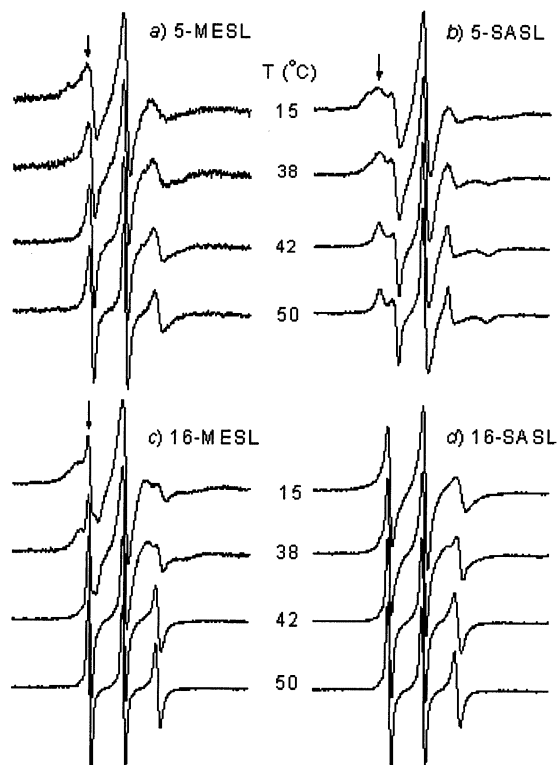


Fig. 7. ESR spectra of spin labels (5- and 16-MESL and SASL) in sonicated DODAB dispersions at different temperatures (15, 38, 42 and 50°C). Total spectra width 100 G. The arrows indicate the low field feature of the more fluid component.

nal at 38°C (Fig. 7(c)), $a_0 \approx 14.46$ G, indicates that this signal is also yielded by the nitroxide moiety inside the hydrophobic bilayer core and not at the bilayer/water interface. Therefore, in sonicated dispersions at temperatures below T_m , a fraction of DODAB molecules are not in the gel phase. The presence of the two populations is clearly observed in the 16-MESL spectrum at 15°C (i.e., far below T_m ; Fig. 7(c); a low field feature of the more isotropic signal is pointed out by the arrow). Though less evident, the two different ESR signals seem to be also present in the spectra yielded by 5-MESL and 5-SASL (arrows in Fig. 7(a) and (b) point to the low field ESR feature related to the fluid phase). It is interesting to note that 16-SASL and 16-MESL partition differently among the diverse structural domains present in the DODAB sonicated dispersions. Indeed, the more polar stearic label is mostly incorporated in the less packed lipid domain, yielding an almost pure one-component ESR signal, typical of a rather mobile spin probe, even at 15°C (Fig. 7(d)). Above T_m , at 50°C, similar to the non-sonicated dispersion, the spin labels incorporated in the sonicated DODAB aggregates display ESR spectra that can be interpreted as a one-component signal, typical of a liquid-crystalline sample. Although not discussed here, the results obtained with the four spin labels (5- and 16-SASL and MESL) incorporated in non-sonicated and sonicated DODAC aggregates were found to be very similar to those obtained for DODAB.

It is shown in Fig. 8 that it is possible to decompose the spectrum of 16-MESL in sonicated DODAB dispersions, below the lipid T_m (Fig. 8(a)), in two components: one similar to that obtained with the label in non-sonicated DODAB dispersions (Fig. 8(b)), corresponding to a gel phase (78%), and the other one being a rather mobile signal (22%; Fig. 8(c)).⁴ The comparison

⁴ Spectrum (c) is the resulting signal, $(c) = (a) - 0.78(b)$, after normalizing the areas of the (a) and (b) spectra. The subtraction proceeded by trial and error, judging by eye the quality of the resultant spectrum (Fig. 8(c)), until it looked like a one-component signal and could be reasonably fitted by a Voigt line shape (Bales, 1989). Here, again, the fact that two well-separated spectra are obtained shows that the exchange

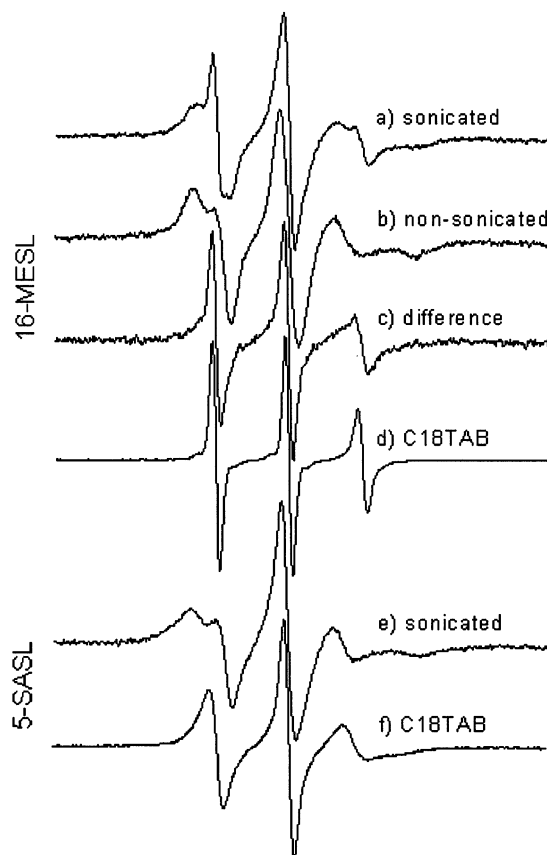


Fig. 8. ESR spectra of 16-MESL in sonicated and non-sonicated DODAB dispersions ((a) and (b), respectively), the resultant spectrum (c) = (a) - 0.78(b) for normalized (a) and (b) second integral values), and in C_{18} TAB micelles (d). ESR spectra of 5-SASL in sonicated DODAB dispersion (e) and in C_{18} TAB micelles (f). Temperature 35°C. Total spectra width 100 G.

of this mobile signal with that yielded by 16-MESL incorporated in C_{18} TAB micelles (Fig. 8(d)), could lead to the conclusion that there are micelles present in the sonicated DODAB dispersions. However, the highly anisotropic spectra yielded by 5-SASL incorporated in the same DODAB sonicated dispersion below T_m (Fig. 8(e)), compared with the rather more isotropic environment felt by 5-SASL in C_{18} TAB micelles (Fig. 8(f)), at the same temperature, indicates that most of the lipid domains monitored in DODAB sonicated dispersion are organized in bilayers and not in micelles.

Similar to the analysis made for the non-sonicated dispersions, the gel to liquid–crystalline phase transition in the sonicated samples can also be monitored by the b/a ratio measured in the 16-MESL ESR spectra, or the line width of the central field line, ΔH_0 , measured in the spectra of both 16-MESL or 16-SASL (Fig. 5). Probably, due to the presence of the two species at low temperatures, the measured phase transition is not so sharp as that observed with the non-sonicated samples (Fig. 6(a)), and can be barely monitored with the ΔH_0 parameter (Fig. 6(b)). Besides, the temperature transition yielded by the b/a ratio (Fig. 6(a)) in sonicated vesicles occurs at about 3°C lower (39°C) than that obtained with the non-sonicated sample (42°C), and no hysteresis could be clearly detected with spin labels. Fluorescent probes have also indicated that in sonicated DODAB dispersions the gel to liquid–crystalline transition is broader and occurs at a lower temperature as compared to the non-sonicated samples (Benatti et al., 1999). However, only the ESR of spin probes can clearly monitor the presence of both the gel and the fluid phases below T_m , in sonicated DODAB and DODAC (not shown) dispersions. It is interesting to point out that the presence of the two phases could possibly explain the different local viscosities measured by the fluorescent and the spin labels in probe-sonicated DODAC dispersions (Liu et al., 1992).

3.3. Comparing the structures of the sonicated and non-sonicated DODAB fluid bilayers

In order to structurally characterize the aggregates present in DODAB dispersions at high temperatures, allowing a comparison between those yielded by non-sonicated and sonicated samples, some spectral parameters of the 16th labeled amphiphiles (16-MESL and 16-SASL) were calculated (Table 2): the correlation times τ_B and τ_C , and the isotropic hyperfine splitting a_0 . (The ESR spectra are typical of the motional narrowing region and can be well fitted with Voigt functions; Bales, 1989; see Section 2). Since the isotropic hyperfine constant a_0 increases with the spin label microenvironment polarity (Griffith et al., 1974), Table 2 shows that the bilayer polarity felt by

both 16-SASL and 16-MESL in DODAB bilayers is rather lower than that felt by the same labels in $C_{18}TAB$ micelles or free in water. Moreover, it is interesting to note that the movement of the spin probes is rather isotropic in water and in the micelles (similar τ_B and τ_C values; see Section 2), and becomes more anisotropic when incorporated in DODAB aggregates.

It is clear that there are structural differences between the aggregates present in sonicated and non-sonicated DODAB dispersions above T_m , as the ESR spectra of the probes in the two preparations are not identical (Table 2, and Figs. 2 and 6). However, the conclusions concerning the packing of the aggregates present in the two differently prepared dispersions are not straightforward, and may depend on the probe localization. For instance, 16-MESL monitors very similar lipid domains in non-sonicated and sonicated samples (similar τ_B , τ_C , and a_0 values for the two samples, see Table 2), whereas 16-SASL monitors more tightly packed (higher correlation times) and more polar (higher a_0 value) lipid domains in the sonicated DODAB sample (Table 2). In addition, the 5-SASL spectra are rather similar for the two DODAB preparations (the bottom spectra in Fig. 3(b) and Fig. 7(b)), while 5-MESL, contrary to 16-SASL, monitors a less packed lipid domain in the sonicated than in the non-sonicated DODAB dispersion (compare the anisotropy of the bottom spectra in Fig. 3(a) and Fig. 6(a)).

4. Conclusions

Spin labels incorporated in 5 mM DODAB aqueous dispersions indicate that both non-sonicated and bath-sonicated aggregates are mostly organized in bilayers, presenting a well-defined gel to liquid–crystalline phase transition. The lower T_m value yielded by the sonicated samples (39.5°C), compared to the non-sonicated (42.7°C), is in accordance with the presence of smaller vesicles in the former (Feitosa and Brown, 1997; Benatti et al., 1999). Chemically distinct spin labels partition differently among structurally distinct DODAB bilayer domains, therefore monitoring several local environments in the bi-

layer, giving comprehensive information about the system. The time-scale of the ESR spectroscopy, together with its high sensitivity to bilayer viscosity, were also essential for the detection of the coexistence of the gel and liquid-crystalline phases in sonicated and non-sonicated dispersions, at temperatures below or around T_m , respectively. To our best knowledge, ESR of spin labels is the first technique capable of detecting the coexistence of the two phases in DODAX bilayer systems. Below T_m , in sonicated dispersions, DODAX molecules in the liquid-crystalline state could be present in vesicles with high curvature, in the periphery of bilayer fragments (Feitosa and Brown, 1997), or in non-smoothed (lens-like) vesicle structures (Andersson et al., 1995). The presence of a fluid phase in DODAX bilayers below or around T_m , may be important for the different characteristics attributed to these synthetic amphiphilic aggregates, for instance, for the efficient incorporation of proteins or DNA (Lasic, 1993; Carvalho and Carmona-Ribeiro, 1998; Kikuchi and Carmona-Ribeiro, 2000), or peculiar reactions found for bilayer adsorbed molecules (Kawamuro et al., 1991; Andersson et al., 1995).

Acknowledgements

This work was supported by USP, FAPESP and CNPq. Fellowships for R.M.F. and C.R.B. (FAPESP) and M.T.L.F. (CNPq, research) are acknowledged.

References

- Andersson, M., Hammarström, L., Edwards, K., 1995. Effect of bilayer phase transitions on vesicle structure and its influence on the kinetics of viologen reduction. *J. Phys. Chem.* 99, 14531–14538.
- Bales, B.L., 1989. Inhomogeneously broadened spin-label spectra. In: Berliner, L.J., Reuben, J. (Eds.), *Spin Labeling. Theory and Applications*, vol. 8. Plenum Press, New York, pp. 77–130.
- Benatti, C.R., Tiera, M.J., Feitosa, E., Olofsson, G., 1999. Phase behavior of synthetic amphiphile vesicles investigated by calorimetry and fluorescence methods. *Thermochim. Acta* 328, 137–142.
- Blandamer, M.J., Briggs, B., Cullis, P.M., Last, P., Engberts, J.B.F.N., Kacperska, A., 1999. Effects of added urea and alkylureas on gel to liquid-crystal transitions in DOAB vesicles. *J. Therm. Anal. Calorimetry* 55, 29–35.
- Budil, D.E., Lee, S., Saxena, S., Freed, J.H., 1996. Nonlinear-least-squares analysis of slow-motion EPR spectra in one and two dimensions using a modified Levenberg-Marquardt algorithm. *J. Mag. Res.* 120, 155–189.
- Carmona-Ribeiro, A.M., Chaimovich, H., 1983. Preparation and characterization of large dioctadecyldimethylammonium chloride liposomes and comparison with small sonicated vesicles. *Biochim. Biophys. Acta* 733, 172–179.
- Carmona-Ribeiro, A.M., 1992. Synthetic amphiphile vesicles. *Chem. Soc. Rev.* 21, 209–214.
- Carvalho, L.A., Carmona-Ribeiro, A.M., 1998. Interaction between cationic vesicles and serum proteins. *Langmuir* 14, 6077–6081.
- Cuccovia, I.M., Feitosa, E., Chaimovich, H., Sepulveda, L., Reed, W., 1990. Size, electrophoretic mobility and ion dissociation of vesicles prepared with synthetic amphiphiles. *J. Phys. Chem.* 94, 3722–3725.
- Cuccovia, I.M., Sesso, A., Abuin, E.B., Okino, P.F., Tavares, P.G., Campos, J.F.S., Florenzano, F.H., Chaimovich, H., 1997. Characterization of dioctadecyldimethylammonium chloride vesicles prepared by membrane extrusion and dichloromethane injection. *J. Mol. Liquids* 72, 323–336.
- Earle, K.A., Moscicki, J.K., Ge, M., Budil, D.E., Freed, J.H., 1994. 250-GHz electron spin resonance studies of polarity gradients along the aliphatic chains in phospholipid membranes. *Biophys. J.* 66, 1213–1221.
- Engberts, J.B.F.N., Hoekstra, D., 1995. Vesicle-forming synthetic amphiphiles. *Biochim. Biophys. Acta* 1241, 323–340.
- Feitosa, E., Brown, W., 1997. Fragment and vesicle structures in sonicated dispersions of dioctadecyldimethylammonium bromide. *Langmuir* 13, 4810–4816.
- Feitosa, E., Barreleiro, P.C.A., Olofsson, G., 2000. Phase transition in dioctadecyldimethylammonium bromide and chloride vesicles prepared by different methods. *Chem. Phys. Lipids* 105, 210–213.
- Fendler, J.H., 1982. *Membrane Mimetic Chemistry*. Wiley-Interscience, New York.
- Fernandez, R.M., Lamy-Freund, M.T., 2000. Correlation between the effects of a cationic peptide on the hydration and fluidity of anionic lipid bilayers: a comparative study with sodium ions and cholesterol. *Biophys. Chem.* 87, 87–102.
- Freed, J.H., 1976. Theory of slow tumbling ESR spectra for nitroxides. In: Berliner, L.J. (Ed.), *Spin Labeling: Theory and Applications*, vol. 1. Academic Press, New York, pp. 53–132.
- Ge, M., Freed, J.H., 1999. Electron-spin resonance study of aggregation of gramicidin in dipalmitoylphosphatidylcholine bilayers and hydrophobic mismatch. *Biophys. J.* 76, 264–280.
- Griffith, O.H., Dehlinger, P.J., Van, S.P., 1974. Shape of the hydrophobic barrier of phospholipid bilayers (evidence for water penetration in biological membranes). *J. Membrane Biol.* 15, 159–192.

- Gugliotti, M., Politi, M.J., Chaimovich, H., 1998. Phase transition temperature of vesicles determined by surface tension: a fast method. *J. Colloid Interf. Sci.* 198, 1–5.
- Halpern, H.J., Peric, M., Yu, C., Bales, B.L., 1993. Rapid quantitation of parameters from inhomogeneously broadened EPR-spectra. *J. Magn. Reson.* 103, 13–22.
- Hubbell, W.L., McConnell, H.M., 1971. Molecular motion in spin-labeled phospholipids and membranes. *J. Am. Chem. Soc.* 93, 314–326.
- Kawamuro, K., Chaimovich, H., Abuin, E., Lissi, E.A., Cucovia, I., 1991. Evidence that the effects of synthetic amphiphile vesicles on reaction rates depend on vesicle size. *J. Phys. Chem.* 95, 1458–1463.
- Kikuchi, I.S., Carmona-Ribeiro, A.M., 2000. Interactions between DNA and synthetic cationic liposomes. *J. Phys. Chem. B* 104, 2829–2835.
- Kunitake, T., Okahata, Y., 1977. A totally synthetic bilayer membrane. *J. Am. Chem. Soc.* 99, 3860–3861.
- Lasic, D.D., 1993. *Liposomes. From Physics to Applications*. Elsevier, Amsterdam.
- Liu, L., Pansu, R., Roncin, J., Faure, J., Arai, T., Tokumaru, K., 1992. Molecular organization in DODAC membrane fragments. *J. Colloid Interf. Sci.* 148, 118–128.
- Marsh, D., 1981. Electron spin resonance: spin labels. In: Grell, E. (Ed.), *Membrane Spectroscopy*. Springer, Berlin, pp. 51–142.
- Marsh, D., 1989. Experimental methods in spin-label spectral analysis. In: Berliner, L.J., Reuben, J. (Eds.), *Spin Labeling. Theory and Applications*, vol. 8. Plenum Press, New York, pp. 255–303.
- Nascimento, D.B., Rapuano, R., Lessa, M.M., Carmona-Ribeiro, A.M., 1998. Counterion effects on properties of cationic vesicles. *Langmuir* 14, 7387–7391.
- Ptak, M., Egret-Charlier, M., Sanson, A., Boloussa, O., 1980. An NMR study of the ionization of fatty acids, fatty amines and N-acylamino acids incorporated in phosphatidylcholine vesicles. *Biochim. Biophys. Acta* 600, 387–397.
- Schneider, D.J., Freed, J.H., 1989. Calculating slow motional magnetic resonance spectra: a user's guide. In: Berliner, L.J., Reuben, J. (Eds.), *Spin Labeling. Theory and Applications*, vol. 8. Plenum Press, New York, pp. 1–76.
- Schreier, S., Polnaszek, C.F., Smith, I.C.P., 1978. Spin labels in membranes. *Problems in practice. Biochim. Biophys. Acta* 515, 375–436.
- Turchiello, R.F., Juliano, L., Ito, A.S., Lamy-Freund, M.T., 2000. How bradykinin alters the lipid membrane structure. A spin label comparative study with bradykinin fragments and other cations. *Biopolymers* 54, 211–221.